Available online at www.sciencedirect.com

ScienceDirect

IFAC PapersOnLine 58-20 (2024) 53–58

Joint Sensor and Actuator Fault Diagnosis for Autonomous Ships ⋆

Agus Hasan† and Pierluigi Salvo Rossi‡

† *Department of ICT and Natural Sciences*
‡ *Department of Electronic Systems*
Norwegian University of Science and Technology
Ålesund, Norway, (e-mail: agus.hasan,pierluigi.salvorossi@ntnu.no).

Abstract: In this paper, we introduce an innovative approach for joint diagnosis of sensor and actuator faults in autonomous ships, leveraging an adaptive extended Kalman filter enriched with a forgetting factor. The fundamental concept involves filtering and augmenting measurements from the sensor systems into the ships' state space model. This method is designed to enhance the accuracy of the diagnostic process by dynamically adapting to changes in the sensor's behavior over time. To validate the efficacy of our proposed method, we conduct numerical simulations. Through these simulations, we aim to demonstrate the practical applicability and reliability of our approach in real-world scenarios, emphasizing its potential for enhancing the fault diagnosis capabilities of autonomous ships.

Keywords: Autonomous ships, fault diagnosis, adaptive extended Kalman filter.

1. INTRODUCTION

1.1 Motivation

Malfunctions and failures in both sensors and actuators can pose substantial threats to operational safety. Sensors are prone to degradation over time, stemming from wear and tear induced by exposure to harsh environmental conditions, mechanical stress, or chemical corrosion, ultimately resulting in diminished accuracy or complete failure as highlighted by Pan et al. (2021). Additionally, sensors often necessitate periodic calibration for accuracy maintenance, and the absence of such calibration can lead to measurement drift, rendering the collected data unreliable. Furthermore, the reliance of many sensors on electronic components, such as transistors and microchips, introduces the risk of malfunction due to manufacturing defects or electrical issues, potentially rendering the entire sensor non-functional. On the other hand, actuators, involving moving parts, are susceptible to mechanical wear and can succumb to breakdowns caused by friction, stress, and fatigue within their mechanical components. The electronic control systems governing actuators may also experience failures, whether attributable to electrical faults, software bugs, or communication issues between the control unit and the actuator. In scenarios where sensors and actuators play a pivotal role in controlling safety-critical systems, such as in autonomous vessels, failures can pose significant risks to both individuals and the environment (Kordestani et al., 2021; Hasan et al., 2024).

Figure 1 depicts an illustrative schematic diagram highlighting potential sensor and actuator faults that may impact the performance of autonomous ships. In this scenario, the faults can be identified through the computation of the residual, which is the difference between the measured sensor output and the expected model output. Subsequently, an estimation algorithm utilizes this residual, employing calculations for state and fault gains. These computations enable the algorithm to estimate the magnitude of both sensor and actuator faults, contributing to the diagnosis and assessment of the overall system performance. This method aids in identifying and addressing potential issues that could affect the autonomy and reliability of the ships.

1.2 Related Works

Fault diagnosis is crucial for maintaining the reliability and performance of autonomous ships. Timely detection and resolution of faults are essential to prevent system failures through fault-tolerant control, minimize downtime, and optimize operational efficiency (Blanke and Nguyen, 2018). Fault diagnosis can be approached through three methods: data-driven, model-based, or a hybrid of both (Darvishi et al., 2021, 2023b). In data-driven fault diagnosis, extensive datasets from embedded sensors are analyzed using machine learning algorithms, such as neural networks and support vector machines (Diget et al., 2022; Gonzalez-Jimenez et al., 2021; Lei et al., 2020; Darvishi et al., 2023a). The goal is to identify patterns in the data that indicate potential faults, allowing for automated anomaly detection and timely intervention. However, challenges include managing large volumes of data, ensuring data quality, and interpreting complex data patterns (Molnar et al., 2020). The success of data-driven fault diagnosis depends on continuous improvement and adaptation of machine learning models to evolving datasets, integrating them effectively into the operational context (Dalzochio et al., 2020). Model-based fault diagnosis constructs a mathematical representation of the systems (Hasan et al.,

⋆ This work is partially supported by Equinor ASA.

10.1016/j.ifacol.2024.10.032

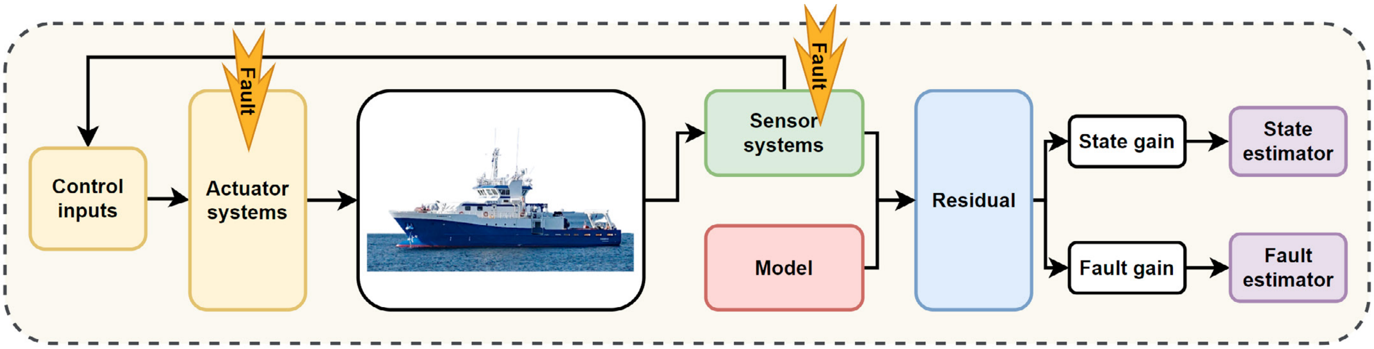

Fig. 1. A schematic representation illustrating the introduction of actuator and sensor faults into autonomous ships.

2023a). This representation, often in the form of mathematical models or equations, captures the expected behavior under normal operating conditions. By comparing predicted behavior with observed behavior, discrepancies serve as indicators of potential faults or anomalies (Schmid et al., 2021). This approach provides detailed insights into system dynamics and facilitates precise fault detection. However, its effectiveness relies on the accuracy of the mathematical model, requiring a thorough understanding of the system's dynamics and continuous maintenance and updating of the model over time. Model-based fault diagnosis may face challenges in capturing complex and dynamic behaviors accurately (Habibi et al., 2019). Hybrid fault diagnosis integrates aspects of both data-driven and model-based methodologies to create a more robust system (Wilhelm et al., 2021; Hasan et al., 2023c,b). This approach leverages the flexibility of data-driven techniques for analyzing vast datasets and identifying patterns, while incorporating structured insights from model-based methods. The combination aims to enhance fault diagnosis performance, especially in scenarios where developing comprehensive models is challenging or data is inherently noisy and complex. In a hybrid system, machine learning algorithms analyze sensor data, while a mathematical model provides structured insights into system dynamics. The synergy achieved is advantageous in addressing real-world complexities, improving accuracy, and maintaining overall system reliability. However, implementing a hybrid fault diagnosis system requires careful consideration of integration between data-driven and model-based components, emphasizing attention to system architecture, algorithm selection, and continuous validation. Despite challenges, the hybrid approach holds promise in fault diagnosis research, offering a versatile solution for diverse operational scenarios (Bhagavathi et al., 2023; Jin et al., 2023).

1.3 Contribution of this Paper

This paper introduces an innovative method contributing to the joint diagnosis of sensor and actuator faults in autonomous systems, employing a hybrid approach that integrates both model-based and data-driven elements. The hybrid approach combines the strengths of models and data for a more comprehensive fault diagnosis strategy. In pursuit of this, we present the development of an adaptive extended Kalman filter algorithm enhanced with a forgetting factor. This adaptive filter is designed to estimate the magnitude of faults in both sensors and actuators, providing a robust and accurate diagnostic tool for ensuring the reliability and performance of autonomous systems. Numerical simulations are presented to demonstrate the efficacy of the proposed method.

1.4 Organization of this Paper

The structure of this paper unfolds as follows. Section 1 encompasses the motivation, related works, and the contributions made in this paper. Formulation of the problem is addressed in Section 2. The fault diagnosis algorithm based on the adaptive extended Kalman filter is detailed in Section 3. Section 4 provides insights into the numerical simulation, while the concluding remarks are presented in Section 5.

2. PROBLEM FORMULATION

In this section, we delve into the exploration of dynamic models that capture the behavior of autonomous ships. These models are mathematically formulated as the following systems:

$$\boldsymbol{x}_k = \boldsymbol{A}_k \boldsymbol{x}_{k-1} + \boldsymbol{f}(\boldsymbol{x}_{k-1}) + \boldsymbol{B}_k \boldsymbol{u}_k + \boldsymbol{\Phi}_k \boldsymbol{\theta}_a + \boldsymbol{w}_k \quad (1)$$

$$\boldsymbol{y}_k = \boldsymbol{C}_k \boldsymbol{x}_k + \boldsymbol{\Psi}_k \boldsymbol{\theta}_s + \boldsymbol{v}_k \quad (2)$$

Here, $\boldsymbol{x}_k \in \mathbb{R}^n$ represents the state vector at time step k, which evolves based on a dynamic matrix $\boldsymbol{A}_k \in \mathbb{R}^{n\times n}$, a nonlinear function $\boldsymbol{f} \in \mathbb{R}^n$, a control input $\boldsymbol{u}_k \in \mathbb{R}^p$, an actuator fault matrix $\boldsymbol{\Phi}_k \in \mathbb{R}^{n\times p}$, and additive noise $\boldsymbol{w}_k \in \mathbb{R}^n$. The output vector $\boldsymbol{y}_k \in \mathbb{R}^m$ is obtained by applying a measurement matrix $\boldsymbol{C}_k \in \mathbb{R}^{m\times n}$ to the state vector $\boldsymbol{x}_k$, augmented by a sensor fault matrix $\boldsymbol{\Psi}_k \in \mathbb{R}^{m\times m}$ and measurement noise $\boldsymbol{v}_k \in \mathbb{R}^m$.

If $\boldsymbol{\Phi}_k = -\boldsymbol{B}_k \mathrm{diag}(\boldsymbol{u}_k)$, then the actuator fault parameter $\boldsymbol{\theta}_a \in \mathbb{R}^p$ can be conceptualized as indicative of a loss in control effectiveness within the autonomous ship system. This parameter captures deviations from the expected performance of the actuators, signifying potential impairments in the ability to manipulate and guide the ship's movements accurately. On the other hand, the sensor fault parameter $\boldsymbol{\theta}_s \in \mathbb{R}^m$ encompasses a broader spectrum of potential issues. It can arise from various sources, including drift, bias, noise, and freeze. Drift refers to gradual and systematic shifts in sensor readings over time, introducing inaccuracies in measurements. Bias represents persistent offsets in sensor outputs from their true values, influencing the overall accuracy of the data. Noise manifests as random fluctuations in sensor readings, contributing to uncertainty and potential misinterpretation of the environment. Freeze denotes a temporary cessation or unresponsiveness in sensor functionality, further complicating the accurate perception of the ship's surroundings. These fault parameters play a critical role in characterizing and quantifying the deviations from the expected behavior of both actuators and sensors. Understanding the implications of $\boldsymbol{\theta}_a$ and $\boldsymbol{\theta}_s$ allows for a comprehensive assessment of potential challenges and vulnerabilities in the autonomous ship system. Addressing and mitigating these fault parameters become paramount in ensuring the reliability and precision of the ship's operations, particularly in dynamic and unpredictable maritime environments. The idea of this paper is to introduce a methodology designed to precisely estimate the magnitude of the identified fault. The primary objective is to provide a robust and accurate assessment of the fault's intensity or extent, allowing for a comprehensive understanding of its impact on the system.

To this end, let us augmenting the filtered measurement sensor:

$$\begin{aligned}\boldsymbol{z}_k = &\boldsymbol{A}_f \Delta t \boldsymbol{C}_k \boldsymbol{x}_{k-1} + (\boldsymbol{I} - \boldsymbol{A}_f \Delta t)\, \boldsymbol{z}_{k-1} \\ &+ \boldsymbol{A}_f \Delta t \boldsymbol{\Psi}_k \boldsymbol{\theta}_s + \boldsymbol{A}_f \Delta t \boldsymbol{v}_k \end{aligned} \tag{3}$$

where the filtering matrix $\boldsymbol{A}_f \in \mathbb{R}^{m\times m}$ is a positive definite matrix and Δt is the sampling time, into (1) and denoting:

$$\boldsymbol{\xi}_k = \begin{pmatrix}\boldsymbol{x}_k \\ \boldsymbol{z}_k\end{pmatrix} \in \mathbb{R}^{n+m} \text{ and } \boldsymbol{\theta} = \begin{pmatrix}\boldsymbol{\theta}_a \\ \boldsymbol{\theta}_s\end{pmatrix} \in \mathbb{R}^{p+m} \tag{4}$$

which yields:

$$\boldsymbol{\xi}_k = \mathcal{A}_k \boldsymbol{\xi}_{k-1} + \mathcal{F}(\boldsymbol{\xi}_{k-1}) + \mathcal{B}_k \boldsymbol{u}_k + \bar{\boldsymbol{\Psi}}_k \boldsymbol{\theta} + \bar{\boldsymbol{w}}_k \tag{5}$$

$$\mathcal{Y}_k = \mathcal{C}_k \boldsymbol{\xi}_k \tag{6}$$

where:

$$\mathcal{A}_k = \begin{pmatrix}\boldsymbol{A}_k & \boldsymbol{0} \\ \boldsymbol{A}_f \Delta t \boldsymbol{C}_k & \boldsymbol{I} - \boldsymbol{A}_f \Delta t\end{pmatrix} \in \mathbb{R}^{(n+m)\times(n+m)} \tag{7}$$

$$\mathcal{F}(\boldsymbol{\xi}_{k-1}) = \begin{pmatrix}\boldsymbol{f}(\boldsymbol{x}_{k-1}) \\ \boldsymbol{0}\end{pmatrix} \in \mathbb{R}^{n+m} \tag{8}$$

$$\mathcal{B}_k = \begin{pmatrix}\boldsymbol{B}_k \\ \boldsymbol{0}\end{pmatrix} \in \mathbb{R}^{(n+m)\times p} \tag{9}$$

$$\bar{\boldsymbol{\Psi}}_k = \begin{pmatrix}\boldsymbol{\Phi}_k & \boldsymbol{0} \\ \boldsymbol{0} & \boldsymbol{A}_f \Delta t \boldsymbol{\Psi}_k\end{pmatrix} \in \mathbb{R}^{(n+m)\times(p+m)} \tag{10}$$

$$\bar{\boldsymbol{w}}_k = \begin{pmatrix}\boldsymbol{w}_k \\ \boldsymbol{A}_f \Delta t \boldsymbol{v}_k\end{pmatrix} \sim \mathcal{N}(\boldsymbol{0}, \mathcal{Q}_k) \in \mathbb{R}^{n+m} \tag{11}$$

$$\mathcal{C}_k = (\boldsymbol{0}\ \ \boldsymbol{I}) \in \mathbb{R}^{m\times(n+m)} \tag{12}$$

The augmented system represented by equations (5)-(6) demonstrates the incorporation of sensor fault within the state space model. This integration provides a comprehensive perspective by encapsulating both sensor and actuator faults. In the subsequent section, we introduce a robust algorithm designed to estimate the magnitude of $\boldsymbol{\theta}$ in (5). Notably, this parameter encompasses the combined influence of sensor and actuator faults, enabling a more holistic and accurate assessment of the system's behavior.

3. JOINT FAULT DIAGNOSIS ALGORITHM

In this section, we introduce a robust algorithm designed for estimating the magnitude of both sensor and actuator faults by leveraging an adaptive extended Kalman filter with a forgetting factor. The algorithm represents a versatile and effective tool for fault diagnosis in systems where real-time adjustments are crucial for maintaining accurate estimations of sensor and actuator faults. To simplify the problem, first we linearize the nonlinear function (1) and define the following linearized matrix:

$$\mathbf{F}_k = \mathcal{A}_k + \left.\frac{\partial \boldsymbol{f}(\boldsymbol{\xi}_k)}{\partial \boldsymbol{\xi}_k}\right|_{\hat{\boldsymbol{\xi}}_{k-1|k-1}} \tag{13}$$

where the last term in the right hand side is simply the Jacobian matrix of $\boldsymbol{f}$. Modifying the adaptive Kalman filter for linear systems presented by Zhang (2018), the fault parameter and state estimators are given as follow:

$$\hat{\boldsymbol{\theta}}_k = \hat{\boldsymbol{\theta}}_{k-1} + \boldsymbol{\Theta}_k \tilde{\mathcal{Y}}_k \tag{14}$$

$$\begin{aligned}\hat{\boldsymbol{\xi}}_{k|k} = &\mathcal{A}_k \hat{\boldsymbol{\xi}}_{k-1|k-1} + \mathcal{F}(\hat{\boldsymbol{\xi}}_{k-1|k-1}) + \mathcal{B}_k \boldsymbol{u}_k + \bar{\boldsymbol{\Psi}}_k \hat{\boldsymbol{\theta}}_{k-1} \\ &+ \boldsymbol{K}_k \tilde{\mathcal{Y}}_k + \boldsymbol{\Pi}_k \left[\hat{\boldsymbol{\theta}}_k - \hat{\boldsymbol{\theta}}_{k-1}\right]\end{aligned} \tag{15}$$

The aforementioned estimators incorporate three distinct gains: $\boldsymbol{\Theta}_k$, $\boldsymbol{K}_k$, and $\boldsymbol{\Pi}_k$. These gains play pivotal roles in shaping the behavior and accuracy of the estimation process, each serving a unique purpose in refining the estimation of fault parameters and system states. The gains can be obtained from the following recursion:

$$\boldsymbol{P}_{k|k-1} = \mathbf{F}_k \boldsymbol{P}_{k-1|k-1} \mathbf{F}_k^\intercal + \mathcal{Q}_k \tag{16}$$

$$\boldsymbol{\Sigma}_k = \mathcal{C}_k \boldsymbol{P}_{k|k-1} \mathcal{C}_k^\intercal \tag{17}$$

$$\boldsymbol{K}_k = \boldsymbol{P}_{k|k-1} \mathcal{C}_k^\intercal \boldsymbol{\Sigma}_k^{-1} \tag{18}$$

$$\boldsymbol{P}_{k|k} = [\boldsymbol{I} - \boldsymbol{K}_k \mathcal{C}_k]\, \boldsymbol{P}_{k|k-1} \tag{19}$$

$$\boldsymbol{\Pi}_k = [\boldsymbol{I} - \boldsymbol{K}_k \mathcal{C}_k]\, \mathbf{F}_k \boldsymbol{\Pi}_{k-1} + [\boldsymbol{I} - \boldsymbol{K}_k \mathcal{C}_k]\, \bar{\boldsymbol{\Psi}}_k \tag{20}$$

$$\boldsymbol{\Omega}_k = \mathcal{C}_k \mathbf{F}_k \boldsymbol{\Pi}_{k-1} + \mathcal{C}_k \bar{\boldsymbol{\Psi}}_k \tag{21}$$

$$\boldsymbol{\Lambda}_k = [\lambda \boldsymbol{\Sigma}_k + \boldsymbol{\Omega}_k \boldsymbol{S}_{k-1} \boldsymbol{\Omega}_k^\intercal]^{-1} \tag{22}$$

$$\boldsymbol{\Theta}_k = \boldsymbol{S}_{k-1} \boldsymbol{\Omega}_k^\intercal \boldsymbol{\Lambda}_k \tag{23}$$

$$\boldsymbol{S}_k = \frac{1}{\lambda} \boldsymbol{S}_{k-1} - \frac{1}{\lambda} \boldsymbol{S}_{k-1} \boldsymbol{\Omega}_k^\intercal \boldsymbol{\Lambda}_k \boldsymbol{\Omega}_k \boldsymbol{S}_{k-1} \tag{24}$$

The initial set of four equations represents the conventional Kalman filter algorithm, specifically employed to compute the Kalman gain $\boldsymbol{K}_k$. This gain is pivotal in adjusting the state estimate based on the current measurement innovation, ensuring an optimal balance between the predicted state and the observed measurements. On the other hand, the subsequent equations are tailored to calculate gains associated with the parameter estimation process. These gains incorporate the concept of a forgetting factor λ. The introduction of the forgetting factor is crucial in adapting the algorithm to changing conditions over time and preventing the undue influence of outdated information in the estimation process. By incorporating the forgetting factor λ into the calculations, the algorithm assigns varying weights to historical data, allowing it to selectively retain relevant information while gradually discounting less pertinent observations. This adaptive mechanism enhances the algorithm's ability to track and respond to dynamic changes in the system, contributing to a more robust and accurate estimation of parameters.

The measurement error $\tilde{\mathcal{Y}}_k$ is obtained from the following expression:

$$\tilde{\mathcal{Y}}_k = \mathcal{Y}_k - \mathcal{C}_k \Big[\mathcal{A}_k \hat{\boldsymbol{\xi}}_{k-1|k-1} + \mathcal{F}(\hat{\boldsymbol{\xi}}_{k-1|k-1}) + \mathcal{B}_k \boldsymbol{u}_k + \bar{\boldsymbol{\Psi}}_k \hat{\boldsymbol{\theta}}_{k-1}\Big] \tag{25}$$

The successful convergence of the fault estimate relies on the continuous excitation of the sequence $\bar{\boldsymbol{\Psi}}_k$. In this context, convergence is achieved when there are fixed positive constants κ and ξ that satisfy the following condition:

$$0 < \kappa \boldsymbol{I} \leq \Sigma_{l=k-\xi}^{k} \bar{\boldsymbol{\Psi}}_l^{\mathsf{T}} \bar{\boldsymbol{\Psi}}_l \tag{26}$$

This requirement ensures that the cumulative inner product of the sequence $\bar{\boldsymbol{\Psi}}_k$ within the defined range remains sufficiently distant from zero, thereby ensuring the necessary excitation for the successful convergence of parameter estimates. Building on the derivation by Zhang (2018), the satisfaction of (26) indicates that the mathematical expectations of the estimation errors:

$$\lim_{k\to\infty} \mathbb{E}(\boldsymbol{\xi}_k - \hat{\boldsymbol{\xi}}_{k|k}) = 0 \tag{27}$$

$$\lim_{k\to\infty} \mathbb{E}(\boldsymbol{\theta}_k - \hat{\boldsymbol{\theta}}_k) = 0 \tag{28}$$

In summarizing the joint fault diagnosis method, we present the algorithm as follows:

Algorithm 1 Pseudo-code for joint sensor and actuator fault diagnosis for autonomous ships

1: **procedure** JointFaultDiagnosis($\hat{\boldsymbol{\xi}}_{k|k}, \hat{\boldsymbol{\theta}}_k$)
2: Initialization:
$\boldsymbol{P}_{0|0} > 0 \in \mathbb{R}^{(n+m)\times(n+m)}$
$\boldsymbol{\Pi}_0 \in \mathbb{R}^{(n+m)\times(p+m)}$
$\boldsymbol{S}_0 = \omega \boldsymbol{I} \in \mathbb{R}^{p+m}$
$\hat{\boldsymbol{\theta}}_0 \in \mathbb{R}^{p+m}$
$\hat{\boldsymbol{\xi}}_{0|0} \in \mathbb{R}^{n+m}$
$\mathcal{Q}_k \in \mathbb{R}^{(n+m)\times(n+m)}$
$\lambda \in \mathbb{R}(0,1)$
$\boldsymbol{A}_f > 0 \in \mathbb{R}^{m\times m}$
3: **for** $k = 0, 1, 2, \cdots$ **do**
4: Calculate $\boldsymbol{\Theta}_k$, $\boldsymbol{K}_k$, and $\boldsymbol{\Pi}_k$ based on (16)-(24).
5: Calculate $\hat{\boldsymbol{\xi}}_{k|k}$ and $\hat{\boldsymbol{\theta}}_k$ based on (14)-(15).
6: **end for**
7: **end procedure**

4. NUMERICAL SIMULATIONS

In this section, we perform system modeling and numerical simulation. The latter is executed using a model of a small unmanned surface vessel (ASV) named Otter, which has been developed by Maritime Robotics. The Otter, designed as a catamaran ASV (depicted in Figure 2), is equipped with electric thrusters powered by up to four interchangeable battery packs. Matlab code for the simulations is available here: `https://github.com/agushasan/sensorandactuatorfaults/`.

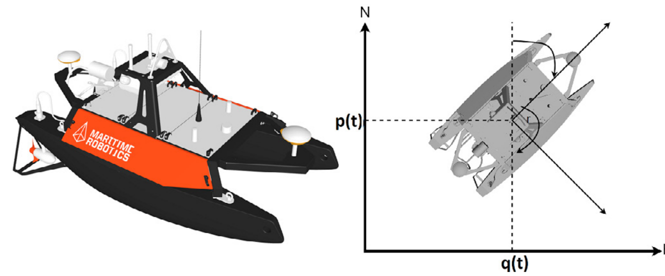

Fig. 2. The Otter (left) and its coordinate modelling.

Positioned at the rear of the vehicle are two fixed propellers that contribute to its motion. Despite its capability for diverse maneuvers, the Otter is classified as underactuated, as it possesses fewer actuators than degrees of freedom. The forward propulsion of the ASV requires both propellers to generate equal thrust. Conversely, differential thrusts from the propellers enable left or right maneuvers, demonstrating the dynamic control capabilities of the vehicle. The integration of these components enables us to establish a robust representation of the system and simulate its behavior under faulty conditions. This approach ensures a thorough and reliable analysis, aligning theoretical modeling with empirical evidence derived from practical applications involving the Otter ASV. The Otter dynamics can be described using the following ordinary differential equations:

$$\dot{p}(t) = U(t)\cos(\chi(t)) + w_1(t) \tag{29}$$

$$\dot{q}(t) = U(t)\sin(\chi(t)) + w_2(t) \tag{30}$$

$$\dot{U}(t) = a(t) + w_3(t) \tag{31}$$

$$\dot{\chi}(t) = r(t) + w_4(t) \tag{32}$$

These equations encapsulate the temporal evolution of fundamental state variables. In this context, $p(t)$ and $q(t)$ symbolize the spatial coordinates of the ASV, $U(t)$ represents its velocity, and $\chi(t)$ describes its heading angle. The variables $a(t)$ and $r(t)$ signify the acceleration and rate of course angle, respectively, and are regarded as the control inputs. The inclusion of noises $w_1(t)$, $w_2(t)$, $w_3(t)$, and $w_4(t)$ is introduced to model inaccuracies within the system. This modeling framework serves as the basis for conducting numerical simulations and subsequent analysis, facilitating a deeper understanding and prediction of the Otter ASV's behavior under varying conditions. We assume we can measure all variables using the sensor system, such that the measurement matrix is given by $\boldsymbol{C} = \boldsymbol{I}_4$.

The augmented fault parameter in sensor and actuator is denoted by:

$$\boldsymbol{\theta} = (\theta_1^a \;\; \theta_2^a \;\; \theta_1^s \;\; \theta_2^s \;\; \theta_3^s \;\; \theta_4^s)^{\mathsf{T}} \in \mathbb{R}^6 \tag{33}$$

In this context, the parameters θ_1^a and θ_2^a exert an influence on the control inputs $a(t)$ and $r(t)$, respectively. Simultaneously, the parameters θ_1^s, θ_2^s, θ_3^s, and θ_4^s have an impact on the sensor inputs corresponding to $p(t)$, $q(t)$, $U(t)$, and $\chi(t)$, respectively. In essence, θ_1^a and θ_2^a contribute to shaping the behavior of the control inputs, while θ_1^s, θ_2^s, θ_3^s, and θ_4^s influence the sensor inputs associated with various state variables. By discretizing the Otter model represented by equations (29)-(32), introducing fault parameters $\boldsymbol{\theta}$, and incorporating the filtered measurement equation into the model, we derive:

$$p_k = p_{k-1} + \Delta t U_{k-1}\cos(\chi_{k-1}) + \Delta t w_k^1 \quad (34)$$
$$q_k = q_{k-1} + \Delta t U_{k-1}\sin(\chi_{k-1}) + \Delta t w_k^2 \quad (35)$$
$$U_k = U_{k-1} + \Delta t(1-\theta_1^a)a_k + \Delta t w_k^3 \quad (36)$$
$$\chi_k = \chi_{k-1} + \Delta t(1-\theta_2^a)r_k + \Delta t w_k^4 \quad (37)$$
$$z_k^1 = 4\Delta t p_{k-1} + (1-4\Delta t)z_{k-1}^1 + 4\Delta t\theta_1^s + 4\Delta t v_k^1 \quad (38)$$
$$z_k^2 = 4\Delta t q_{k-1} + (1-4\Delta t)z_{k-1}^2 + 4\Delta t\theta_2^s + 4\Delta t v_k^2 \quad (39)$$
$$z_k^3 = 4\Delta t U_{k-1} + (1-4\Delta t)z_{k-1}^3 + 4\Delta t\theta_3^s + 4\Delta t v_k^3 \quad (40)$$
$$z_k^4 = 4\Delta t \chi_{k-1} + (1-4\Delta t)z_{k-1}^4 + 4\Delta t\theta_4^s + 4\Delta t v_k^4 \quad (41)$$

Here, for pedagogical consideration we select $\boldsymbol{A}_f = 4\boldsymbol{I}$. The discrete-time representation (34)-(41) resembles (1) with:

$$\mathcal{A}_k = \begin{pmatrix} \boldsymbol{I} & \boldsymbol{0} \\ 4\Delta t\boldsymbol{I} & \boldsymbol{I} - 4\Delta t\boldsymbol{I} \end{pmatrix} \in \mathbb{R}^{8\times 8} \quad (42)$$

$$\mathcal{F}(\boldsymbol{\xi}_{k-1}) = \begin{pmatrix} \Delta t U_{k-1}\cos(\chi_{k-1}) \\ \Delta t U_{k-1}\sin(\chi_{k-1}) \\ \boldsymbol{0} \end{pmatrix} \in \mathbb{R}^{8} \quad (43)$$

$$\mathcal{B}_k = \begin{pmatrix} \boldsymbol{B} \\ \boldsymbol{0} \end{pmatrix} \in \mathbb{R}^{8\times 2} \quad (44)$$

$$\boldsymbol{B} = \begin{pmatrix} 0 & 0 & \Delta t & 0 \\ 0 & 0 & 0 & \Delta t \end{pmatrix}^{\mathsf{T}} \in \mathbb{R}^{4\times 2} \quad (45)$$

$$\bar{\boldsymbol{\Psi}}_k = \begin{pmatrix} -\boldsymbol{B}\mathrm{diag}(\boldsymbol{u}_k) & \boldsymbol{0} \\ \boldsymbol{0} & 4\Delta t\boldsymbol{I} \end{pmatrix} \in \mathbb{R}^{8\times 6} \quad (46)$$

$$\bar{\boldsymbol{w}}_k = \begin{pmatrix} \Delta t\boldsymbol{w}_k \\ 4\Delta t\boldsymbol{v}_k \end{pmatrix} \sim \mathcal{N}(\boldsymbol{0}, \mathcal{Q}_k \in \mathbb{R}^8) \quad (47)$$

Utilizing the joint fault estimation algorithm detailed in Section 3, the resulting estimated state under sensor and actuator faults is illustrated in Figure 3. The visualization provides insights into the impact of faults on the trajectory, velocity, and course angle of the autonomous ships. Examining Figure 3, it becomes evident how sensor and actuator faults influence the behavior of the autonomous ships. The trajectory, velocity, and course angle exhibit deviations from the expected values due to the introduced faults. This visual representation not only highlights the efficacy of the joint fault estimation algorithm in capturing and quantifying these deviations but also offers a tangible depiction of the disturbances caused by sensor and actuator faults in the autonomous ship dynamics. The analysis of such visualizations plays a crucial role in understanding the algorithm's performance and its ability to mitigate the effects of faults on the system. Note that our proposed Algorithm 1 involves two primary tuning parameters: the forgetting factor λ and the filtering matrix $\boldsymbol{A}_f$. In the subsequent simulations, we examine the impact of these tuning parameters on the estimation process.

By manipulating the value of the forgetting factor λ, as can be seen from Figure 4, the fault estimation exhibits varying transient responses. Notably, a higher value of λ corresponds to a reduced overshoot in the fault estimation; however, it comes at the expense of a slower response. The forgetting factor λ plays a crucial role in influencing the

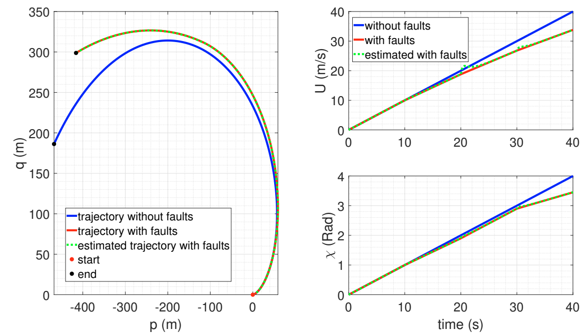

Fig. 3. The evolution of the states under sensor and actuator faults.

algorithm's adaptability to changes in the system. When λ is set to a higher value, the algorithm tends to place greater emphasis on recent measurements, resulting in a more conservative response with lower overshooting tendencies. Conversely, a lower value of λ enables the algorithm to adapt more swiftly to dynamic changes, leading to a faster response but potentially allowing for higher overshoot in the fault estimation. This trade-off between overshoot and response speed underscores the importance of tuning the forgetting factor based on the specific requirements and characteristics of the system.

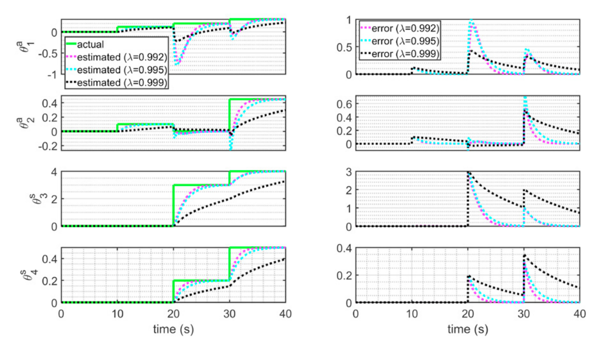

Fig. 4. Fault estimation for different value of λ.

When we vary the eigenvalues of matrix $\boldsymbol{A}_f$, as shown in Figure 5, it becomes evident that higher eigenvalues result in a transient response characterized by a larger overshoot. Conversely, in cases where the eigenvalues of $\boldsymbol{A}_f$ are lower, a more favorable and responsive behavior is observed. The eigenvalues of $\boldsymbol{A}_f$ play a significant role in shaping the dynamics of the system. Higher eigenvalues indicate a faster rate of growth in the system's response, leading to a more pronounced overshoot during the transient phase. On the other hand, lower eigenvalues signify a more subdued response, which often translates to a reduced overshoot but may come at the expense of slower dynamics. In practical terms, the choice of eigenvalues for $\boldsymbol{A}_f$ involves a trade-off between achieving a swift response and minimizing overshoot. Depending on the specific requirements of the system and the desired performance characteristics, selecting lower eigenvalues for $\boldsymbol{A}_f$ can yield a more favorable response, balancing the need for responsiveness without compromising on stability.

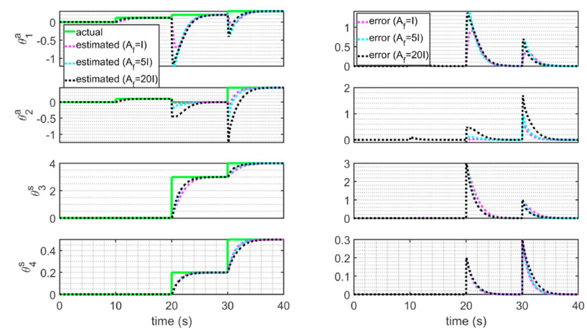

Fig. 5. Fault estimation for different value of $\boldsymbol{A}_f$.

5. CONCLUSION

In this paper, we have introduced a unified hybrid approach algorithm dedicated to joint sensor and actuator fault diagnosis. The algorithm leverages a versatile model capable of detecting faults in both actuator and sensor systems. It is important to highlight that the utilization of higher fidelity models can enhance fault localization precision, allowing the algorithm to be tailored to specific system intricacies. The algorithms are equipped with tuning parameters, providing flexibility for adjustments that contribute to an improved convergence rate, a critical factor in achieving accurate fault diagnosis. Our approach is substantiated through numerical simulations, effectively demonstrating the proficiency of the algorithm in accurately estimating fault magnitudes. The results underscore its robustness across a spectrum of simulated scenarios, affirming its potential suitability for deployment in autonomous systems. Future works will focus on refining and expanding upon the presented algorithms. This includes investigating their adaptability to diverse system architectures and fault types, optimizing tuning parameters for specific applications, and addressing real-time implementation challenges.

REFERENCES

Bhagavathi, R., Kufoalor, D.K.M., and Hasan, A. (2023). Digital twin-driven fault diagnosis for autonomous surface vehicles. *IEEE Access*, 11, 41096–41104.

Blanke, M. and Nguyen, D.T. (2018). Fault tolerant position-mooring control for offshore vessels. *Ocean Engineering*, 148, 426–441.

Dalzochio, J., Kunst, R., Pignaton, E., Binotto, A., Sanyal, S., Favilla, J., and Barbosa, J. (2020). Machine learning and reasoning for predictive maintenance in industry 4.0: Current status and challenges. *Computers in Industry*, 123, 103298.

Darvishi, H., Ciuonzo, D., Eide, E.R., and Salvo Rossi, P. (2021). Sensor-fault detection, isolation and accommodation for digital twins via modular data-driven architecture. *IEEE Sensors Journal*, 21(4), 4827–4838.

Darvishi, H., Ciuonzo, D., and Salvo Rossi, P. (2023a). Deep recurrent graph convolutional architecture for sensor fault detection, isolation, and accommodation in digital twins. *IEEE Sensors Journal*, 23(23), 29877–29891.

Darvishi, H., Ciuonzo, D., and Salvo Rossi, P. (2023b). A machine-learning architecture for sensor fault detection, isolation, and accommodation in digital twins. *IEEE Sensors Journal*, 23(3), 2522–2538.

Diget, E.L., Hasan, A., and Manoonpong, P. (2022). Machine learning with echo state networks for automated fault diagnosis in small unmanned aircraft systems. In *2022 International Conference on Unmanned Aircraft Systems (ICUAS)*, 1066–1072. IEEE.

Gonzalez-Jimenez, D., del Olmo, J., Poza, J., Garramiola, F., and Madina, P. (2021). Data-driven fault diagnosis for electric drives: A review. *Sensors*, 21(12).

Habibi, H., Howard, I., and Simani, S. (2019). Reliability improvement of wind turbine power generation using model-based fault detection and fault tolerant control: A review. *Renewable Energy*, 135, 877–896.

Hasan, A., Asfihani, T., Osen, O., and Bye, R.T. (2024). Leveraging digital twins for fault diagnosis in autonomous ships. *Ocean Engineering*, 292, 116546.

Hasan, A., Tahavori, M., and Midtiby, H.S. (2023a). Model-based fault diagnosis algorithms for robotic systems. *IEEE Access*, 11, 2250–2258.

Hasan, A., Widyotriatmo, A., Fagerhaug, E., and Osen, O. (2023b). Predictive digital twins for autonomous ships. In *2023 IEEE Conference on Control Technology and Applications (CCTA)*, 1128–1133. IEEE.

Hasan, A., Widyotriatmo, A., Fagerhaug, E., and Osen, O. (2023c). Predictive digital twins for autonomous surface vessels. *Ocean Engineering*, 288, 116046.

Jin, H., Gao, Z., Zuo, Z., Zhang, Z., Wang, Y., and Zhang, A. (2023). A combined model-based and data-driven fault diagnosis scheme for lithium-ion batteries. *IEEE Transactions on Industrial Electronics*, 1–11.

Kordestani, M., Saif, M., Orchard, M.E., Razavi-Far, R., and Khorasani, K. (2021). Failure prognosis and applications—a survey of recent literature. *IEEE Transactions on Reliability*, 70(2), 728–748.

Lei, Y., Yang, B., Jiang, X., Jia, F., Li, N., and Nandi, A.K. (2020). Applications of machine learning to machine fault diagnosis: A review and roadmap. *Mechanical Systems and Signal Processing*, 138, 106587.

Molnar, C., Casalicchio, G., and Bischl, B. (2020). Interpretable machine learning – a brief history, state-of-the-art and challenges. In *ECML PKDD 2020 Workshops*, 417–431.

Pan, J., Qu, L., and Peng, K. (2021). Sensor and actuator fault diagnosis for robot joint based on deep cnn. *Entropy*, 23(6).

Schmid, M., Gebauer, E., Hanzl, C., and Endisch, C. (2021). Active model-based fault diagnosis in reconfigurable battery systems. *IEEE Transactions on Power Electronics*, 36(3), 2584–2597.

Wilhelm, Y., Reimann, P., Gauchel, W., and Mitschang, B. (2021). Overview on hybrid approaches to fault detection and diagnosis: Combining data-driven, physics-based and knowledge-based models. *Procedia CIRP*, 99, 278–283.

Zhang, Q. (2018). Adaptive kalman filter for actuator fault diagnosis. *Automatica*, 93, 333–342.